

# Army Research Laboratory

Aberdeen Proving Ground, MD 21005-5066

---

---

ARL-TR-2453

April 2001

---

---

## Theoretical Studies of the Hydrostatic Compression of RDX, HMX, HNIW, and PETN Crystals

Dan C. Sorescu  
Oklahoma State University

Betsy M. Rice  
Weapons and Materials Research Directorate, ARL

Donald L. Thompson  
Oklahoma State University

---

---

## Abstract

---

A previously developed intermolecular potential for nitramines and several other classes of nitrocompound crystals has been used to investigate the behavior of the energetic materials hexahydro-1,3,5-trinitro-1,3,5-*s*-triazine (RDX), 1,3,5,7-tetranitro-1,3,5,7-tetraazacyclo-octane (HMX), 2,4,6,8,10,12-hexanitrohexaazaisowurtzitane (HNIW), and pentaerythritol tetranitrate (PETN) under hydrostatic compression. Isothermal-isobaric molecular simulations (assuming the rigid-molecule approximation) molecular-packing calculations were used to perform the analyses. In the case of the RDX, HMX, and HNIW crystals, the results indicate that the proposed potential model is able to accurately reproduce the changes in the structural crystallographic parameters as functions of pressure for the entire range of pressures that has been investigated experimentally. In addition, the calculated bulk moduli of RDX and HMX were found to be in good agreement with the corresponding experimental results. In the case of the PETN crystal, the crystallographic parameters have been reproduced with an acceptable accuracy at pressures up to about 5 GPa. The larger deviations from the experimental results at greater pressures indicate the limitations of the rigid-molecule model when applied to floppy molecules. The similarity of the results determined in molecular-packing calculations relative to those from molecular dynamics simulations suggest that the former method can be used as an efficient tool for rapid tests of the crystal structure modification under pressure.

## **Acknowledgments**

This work was supported by the Strategic Environmental Research and Development Program (SERDP). Donald L. Thompson gratefully acknowledges support by the U.S. Army Research Office under grant number DAAG55-98-1-0089. We would like to thank Dr. Alan Pinkerton (University of Toledo) for providing his experimental results for  $\epsilon$ -HNIW prior to publication.

INTENTIONALLY LEFT BLANK.

# Table of Contents

	<u>Page</u>
<b>Acknowledgments</b> .....	iii
<b>List of Figures</b> .....	vii
<b>List of Tables</b> .....	ix
<b>1. Introduction</b> .....	1
<b>2. Intermolecular Potential</b> .....	5
<b>3. Computational Approach</b> .....	6
3.1 Molecular Packing Calculations.....	6
3.2 Constant Pressure and Temperature Molecular Dynamics Calculations .....	6
<b>4. Results and Discussions</b> .....	8
4.1 RDX Crystal.....	8
4.2 HMX Crystal .....	12
4.3 HNIW Crystal.....	15
4.4 PETN Crystal .....	15
<b>5. Conclusions</b> .....	21
<b>6. References</b> .....	25
<b>Distribution List</b> .....	29
<b>Report Document Page</b> .....	31

INTENTIONALLY LEFT BLANK.

# List of Figures

<u>Figure</u>	<u>Page</u>
1. Molecular Configurations of (a) RDX ( $\alpha$ -Phase), (b) HMX ( $\beta$ -Phase), (c) HNIW ( $\epsilon$ -Phase), and (d) PETN (Tetragonal Phase) .....	4
2. Comparison of the Crystallographic Parameters Obtained in MP and NPT-MD Simulations for the $\alpha$ -RDX Crystal With the Experimental Results .....	11
3. Comparison of the Crystallographic Parameters Obtained in MP and NPT-MD Simulations for the $\beta$ -HMX Crystal With the Experimental Results .....	14
4. Comparison of the Crystallographic Lattice Dimensions Obtained in MP and NPT-MD Simulations for the $\epsilon$ -HNIW Crystal With the Experimental Results .....	16
5. Comparison of the Crystallographic Parameters Obtained in MP and NPT-MD Simulations for Tetragonal Phase of PETN Crystal With the Experimental Results .....	18
6. The Pressure-Volume Dependence for PETN in the Case of Uniaxial Compression Along the $a$ -Axis and $c$ -Axis, Respectively.....	20
7. Radial Distribution Functions for COM-COM Pairs as Function of Pressure for (a) $\alpha$ -RDX, (b) $\beta$ -HMX, (c) $\epsilon$ -HNIW, and (d) PETN (Tetragonal Phase) .....	22

INTENTIONALLY LEFT BLANK.

## List of Tables

<u>Table</u>		<u>Page</u>
1.	Lattice Parameters Obtained in Crystal Packing and Molecular Dynamics Calculations for the $\alpha$ -RDX Crystal as a Function of Pressure at T = 298 K.....	9
2.	Coefficients of the Quadratic Fits of the Form $a_0 + a_1P + a_2P^2$ for RDX, HMX, and HNIW and of the Cubic Fit of the Form $a_0(1 + a_1P + a_2P^2 + a_3P^3)$ for PETN of the Lattice Constants and Unit Cell Volume as Function of Pressure (GPa) Using Results From the NPT-MD Calculations.....	10
3.	Lattice Parameters Obtained in Crystal Packing and Molecular Dynamics Calculations for the $\beta$ -HMX Crystal as a Function of Pressure at T = 298 K.....	13
4.	Lattice Parameters Obtained in Crystal Packing and Molecular Dynamics Calculations for the $\varepsilon$ -HNIW Crystal as a Function of Pressure at T = 298 K.....	17
5.	Lattice Parameters Obtained in Crystal Packing and Molecular Dynamics Calculations for the PETN Crystal as a Function of Pressure at T = 298 K.....	19

INTENTIONALLY LEFT BLANK.

# 1. Introduction

New strategies for the development of new energetic materials or deployment of existing materials in advanced weapons platforms have incorporated technologies that result in cost and time efficiency. These strategies include modeling and simulation at the various stages in the developmental process. Modeling and simulation are recognized to be a cost-effective and efficient means of achieving such goals in any developmental process. Atomistic simulation for characterization and prediction of physical and chemical behavior of energetic materials promises to be one of the more powerful and effective modeling methodologies that is incorporated into the new developmental strategies. Accurate atomistic predictions provide information of the fundamental mechanisms of processes that determine performance of the materials. However, the effectiveness of the simulations is limited by the accuracy of the description of the interaction potential of the models. An attempt has been made to develop classical models of energetic materials that will accurately reproduce known properties of these materials. The approach has been to first develop simple potential functions to describe the interactions between molecules in the crystals, while the overall goal is to enhance these models such that the accurate description of different complex physical and chemical processes, including chemical reactions in the condensed phase, can be achieved. Since most of the processes of interest here are in the condensed phase and involve systems containing large polyatomic molecules, it is imperative that the interactions are described by simple functions; otherwise atomistic simulation could become computationally intractable. Such simple functions have been developed and have been evaluated in a series of studies that predict crystallographic parameters at ambient conditions [1–5].

An initial study [1] has shown how an atom-atom (6-exp) Buckingham potential with electrostatic interaction terms in the form of partial charges associated with the atoms of the molecules can be parameterized to reproduce the experimental crystal structure of the  $\alpha$ -form of the solid explosive, hexahydro-1,3,5-trinitro-1,3,5-s-triazine (RDX). This intermolecular potential was used to simulate the RDX crystal structure in isothermal-isobaric molecular dynamics (NPT-MD) calculations at ambient pressure and for temperatures ranging from 4.2 to

325 K. The results of the simulations indicated very good agreement with experiment, with the lattice dimensions being within 2% of experiment and almost no rotational or translational disorder of the molecules in the unit cell. The space-group symmetry was maintained throughout the simulations for the average structures. Additionally, the predicted thermal expansion coefficients were in reasonable agreement with experiment.

The utility of the proposed potential was expanded when it was shown that the same Buckingham 6-exp potential terms can be used without modification to characterize (through molecular packing [MP] and NPT-MD simulations) the structures and their thermal dependence for other nitramine crystals (i.e., 2,4,6,8,10,12-hexanitrohexaazaisowurtzitane [HNIW] [2] and 1,3,5,7-tetranitro-1,3,5,7-tetraazacyclo-octane [HMX] [3]). Investigations indicate that this potential predicts accurately not only the crystallographic structures of different phases of these crystals but also the correct lattice energies and the relative order of stability. Particularly, the potential indicate the stability order  $\epsilon > \beta > \gamma$  and  $\beta > \alpha > \delta$  for the corresponding phases of HNIW and HMX, in agreement with the experimental measurements [6, 7].

More recently, investigations of the transferability of this interaction potential in molecular simulations of 30 nitramine crystals [4] have been extended. The molecules associated with the nitramine crystals were chosen as representative examples of acyclic and cyclic nitramines. In the latter case, different types of mono- and polycyclic nitramines have been included, particularly crystals of importance in energetic materials. For most of the crystals, the predicted structural lattice parameters differ by less than 2% from the experimental structures, with small rotations and practically no translations of the molecules in the asymmetric unit cell.

Finally, studies have expanded to assess whether the interaction potential could be used to model crystals beyond the class of nitramines. MP calculations have been performed on 51 crystals comprising a wide variety of compounds such as nitroalkanes, nitroaromatics, nitrocubanes, polynitroadamantanes, polynitropolycycloundecanes, polynitropolycyclododecanes, hydroxy-nitroderivatives, nitrobenzotriles, nitrobenzotriazoles, and nitrate esters, such that a comprehensive test to this potential was achieved [5]. It was shown that, for the majority

of these crystals, the potential model accurately reproduces the crystallographic structural and energetic data determined experimentally. Moreover, in the same study, the temperature dependence of the crystallographic parameters has been analyzed for two important energetic crystals, 2,4,6-trinitrotoluene (TNT) in the monoclinic phase and the pentaerythritol tetranitrate (PETN) crystal in the tetragonal phase. In each case, the results show that, throughout the MD simulations, the average structures of the crystals maintain the same space group symmetry as the one determined experimentally and there is a good agreement between the calculated crystallographic parameters and the experimental values.

The present paper considers another category of tests through which one can assess the quality of the potentials. In particular, focus is on the analysis of the hydrostatic compression of some energetic materials and if the structural changes observed experimentally can be described accurately with the present set of potentials. For this purpose, consideration is given to the case of the nitramine crystals RDX ( $\alpha$ -phase), HMX ( $\beta$ -phase), and HNIW ( $\epsilon$ -phase) and the non-nitramine crystal PETN for which experimental information is available. The configurations of the molecules corresponding to these are illustrated in Figure 1. As can be seen, RDX and HMX have monocyclic molecular configurations, HNIW is polycyclic, and PETN is acyclic.

As in the preceding studies [1–5], the previously presented [1] RDX Buckingham potential was used, plus Coulombic interactions terms obtained through fitting of partial charges centered on each atom of the molecule (in the experimental arrangement) to a quantum mechanically derived electrostatic potential [8]. It has been shown for both the nitramine [4] and non-nitramine [5] crystals that the best agreement between the calculated and experimental energies is obtained when the set of charges is determined using methods that employ electron correlation effects. For example, in the case of a set of 30 nitramine crystals previously analyzed [4], an average deviation of the Hartree-Fock lattice energies of 12.8% was found from the corresponding Möller-Plesset (MP2) [9–12] energies. The use of density functional theory (B3LYP) to evaluate the electrostatic charges decreases these deviations of the lattice energies to about 2.6%. Thus, in the present case, the sets of charges were derived using the second-order Möller-Plesset (MP2) perturbation theory.

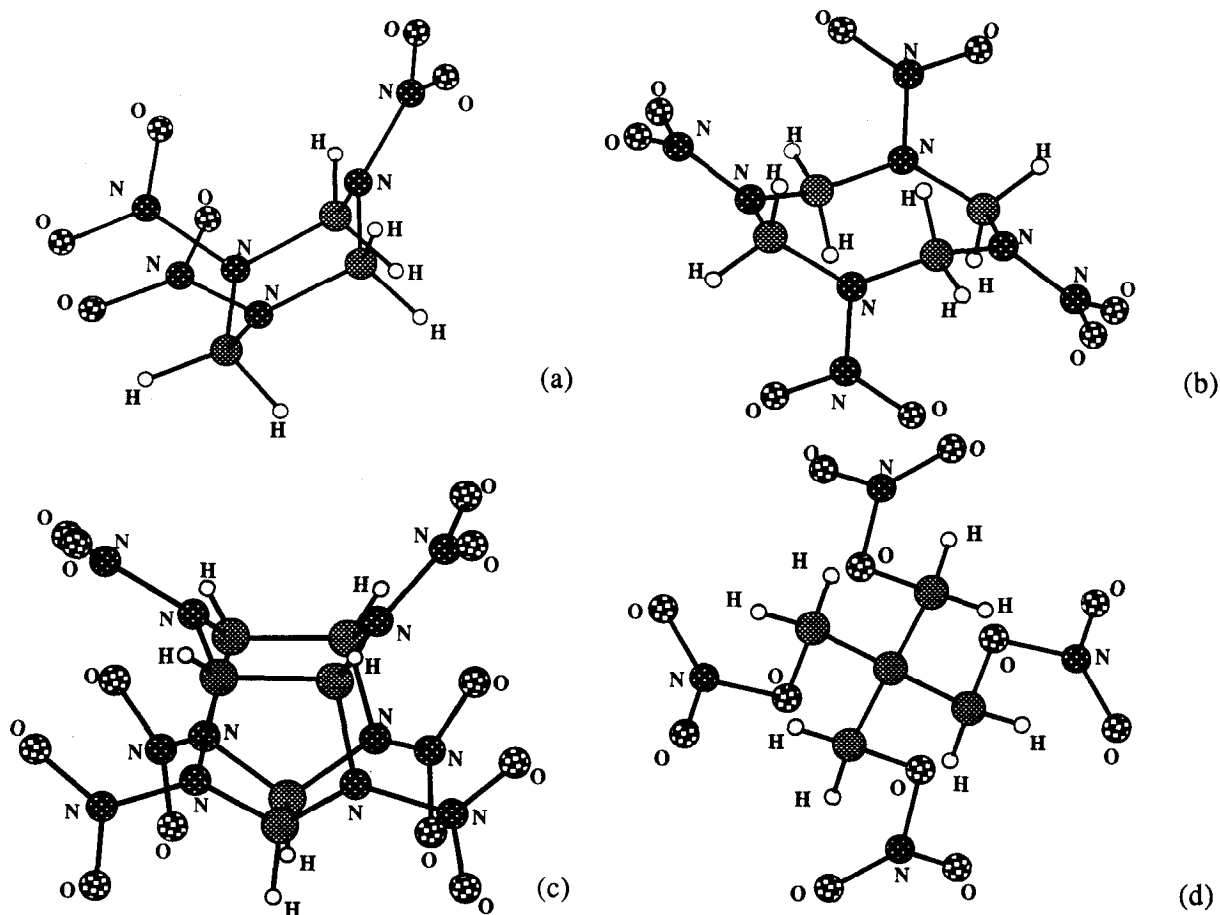


**Figure 1. Molecular Configurations of (a) RDX ( $\alpha$ -Phase), (b) HMX ( $\beta$ -Phase), (c) HNIW ( $\epsilon$ -Phase), and (d) PETN (Tetragonal Phase).**

As in the previous studies [1–5], the main limitation of these models remains the assumption of rigid molecules. However, as previously discussed by Pastine [13], the initial compression of an organic explosive is almost entirely due to a reduction of intermolecular distances. It is only at small intermolecular distances that the increase of van der Waals repulsions become comparable to the intramolecular repulsions along the covalent bonds [13]. Consequently, the assumption of rigid molecules should be adequate in describing the initial compression of such crystals within the regime in which intramolecular deformations are small. This should be valid for the crystals containing molecules that are not very floppy, such as the RDX, HMX, and HNIW crystals. This approach, in which rigid molecules are assumed in simulations of the hydrostatic effects on crystallographic parameters, has also been used previously [14].

The organization of the paper is as follows. In section 2, the intermolecular potential used to simulate the crystals is presented. In section 3, the details of calculations using molecular packing methods and isothermal-isobaric MD calculations are described. The results of these calculations are given in section 4. The main conclusions are summarized in section 5.

## 2. Intermolecular Potential

The intermolecular potential used in the present study is that previously used for nitramine [4] and non-nitramine [5] crystals. Therefore, only brief details are provided. The intermolecular interactions between the molecules of the crystal are approximated by using superpositions of pairwise Buckingham (6-exp) (repulsion and dispersion) and Coulombic (C) potentials of the form

$$V_{\alpha\beta}(r) = A_{\alpha\beta} \exp(-B_{\alpha\beta}r) - C_{\alpha\beta}/r_{\alpha\beta}^6 \quad (1)$$

and

$$V_{\alpha\beta}^C(r) = \frac{q_{\alpha}q_{\beta}}{4\pi\epsilon_0 r} \quad (2)$$

where  $r$  is the interatomic distance between atoms  $\alpha$  and  $\beta$ ,  $q_{\alpha}$  and  $q_{\beta}$  are the electrostatic charges on the atoms, and  $\epsilon_0$  is the dielectric permittivity constant of vacuum.

The parameters for the 6-exp potential in equation (1) are those previously determined for the RDX crystal [1]. The heteroatom parameters are calculated from the homoatom parameters using the same combination rules as previously reported [1].

The assignments of the electrostatic charges were made by using the set of atom-centered monopole charges for the isolated molecule (with the structure fixed at the experimental

crystallographic configuration) that best reproduces the quantum mechanically derived electrostatic potential. The electrostatic potential is calculated over grid points surrounding the van der Waals surface of the molecules. This method of fitting the electrostatic potential was proposed by Breneman and Wiberg [8] and is incorporated in the *Gaussian 94* package of programs [15] under the keyword CHELPG (electrostatic-potential-derived atomic charges). These calculations have been done at MP2 theoretical level using a reasonable quality basis set (i.e., 6-31G\*\* [split-valence plus d-type and p-type polarization functions]) [16].

### 3. Computational Approach

**3.1 Molecular Packing Calculations.** Preliminary tests of the capability of the interaction potential to adequately predict the crystal structural behavior under hydrostatic compression are performed using molecular packing calculations [17, 18], in which the lattice energy of a crystal is minimized with respect to its structural degrees of freedom. These calculations have been done using the algorithm proposed by Gibson and Scheraga [19] for efficient minimization of the energy of a fully variable lattice composed of rigid molecules and implemented in the program LMIN [20]. The nonbonded interactions were attenuated using a cubic spline function from  $P\sigma$  to  $Q\sigma$ , to ensure the continuity of the function and its first derivative. Here  $\sigma$  is the value of  $r$  in equation (1) at which  $V_{\alpha\beta}(r) = 0$  and  $dV_{\alpha\beta}(r)/dr < 0$ . The parameters  $P$  and  $Q$ , which specify the start and the end of the cubic feather (see Sorescu et al. [1] and Desiraju [18] for details) were set to 20.0 and 20.5, respectively. The Coulombic potential terms of the form given in equation (2) are summed over the lattice using the Ewald technique as previously described [1]. Finally, the effect of pressure on the crystallographic parameters has been simulated by adding a potential term of the form  $P(V - V_0)$  [21], where  $V_0$  is the volume of a suitably chosen unit cell at zero pressure.

**3.2 Constant Pressure and Temperature Molecular Dynamics Calculations.** A more comprehensive test of the ability of the interaction potential to predict the crystal structure of the molecular crystals under hydrostatic compression has been done using constant pressure and temperature (NPT) molecular dynamics simulations, in which there are no geometric constraints

other than the assumption of rigid-body molecules. This method yields average equilibrium properties of the lattice as functions of temperature and pressure.

The Nosé-Hoover barostat algorithm [22] has been used as implemented in the program DL\_POLY\_2.0,\* to simulate the crystals at various temperatures and pressures. In this case, the equations of motion for both the translation of rigid molecules and the simulation cell are integrated using the Verlet leap-frog scheme [23]. The molecular rotational motion is handled using Fincham's implicit quaternion algorithm [24].

The MD simulation cells consist of boxes containing  $3 \times 3 \times 3$ ,  $4 \times 2 \times 3$ ,  $3 \times 2 \times 3$ , and  $3 \times 3 \times 4$  crystallographic unit cells for the RDX, HMX, HNIW, and PETN crystals, respectively. These choices of the simulation boxes ensure the use of a cutoff distance for the intermolecular potentials of about 10 Å. For each of the four different molecular crystals, a simulation corresponding to the lowest pressure was first performed, with the position and orientation of the molecules in the unit cell initially set to be identical to those for the experimental structure. The systems were then equilibrated at 298 K and atmospheric pressure. In all production runs, the total integration time corresponded to 12,000 time steps (1 time step =  $2 \times 10^{-15}$  s), of which 2,000 steps were equilibration. The velocities were scaled after every five steps during the equilibration period so that the internal temperature of the crystal mimicked the imposed external temperature. Properties were then calculated and accumulated for averaging over the next 1,0000 integration steps in the simulation. In subsequent runs, performed at successively higher pressures and a constant temperature of 298 K, the initial configurations of the molecular positions and velocities were those corresponding to the final values from the preceding lower-pressure simulation.

The lattice sums were calculated subject to the use of minimum-image periodic boundary conditions in all dimensions [23]. The interactions were determined between the sites (atoms) in the simulation box and the nearest-image sites within the cutoff distance. In these calculations, the Coulombic long-range interaction were handled using Ewald's method [23].

---

\* DL\_POLY is a package of molecular simulation routines written by W. Smith and T. R. Forester, copyright The Council for the Central Laboratory of the Research Councils, Daresbury Laboratory at Daresbury, Nr., Warrington, 1996.

The main quantities obtained from these simulations were the average lattice dimensions and the corresponding volume of the unit cell. Additional information about the structure of the crystal has been obtained by calculating the center-of-mass (COM)-COM radial distribution functions (RDF). Such quantities have been calculated from recordings done at every 10th step during trajectory integrations.

## 4. Results and Discussions

**4.1 RDX Crystal.** Crystalline RDX exists in two phases [25]: the ambient phase ( $\alpha$ -solid), for which the structure has been characterized by neutron diffraction measurements [26], and an unstable phase ( $\beta$ -solid), the crystal structure of which has not been determined. The structure of  $\alpha$ -RDX at room temperature and 1-atm pressure belongs to the orthorhombic space group  $Pbca$  with  $Z = 8$  molecules per unit cell. The linear and volume compression of RDX have been investigated by Olinger et al. [27] for pressures up to 9 GPa using a high-pressure x-ray diffraction technique. It has shown that the ambient RDX polymorph is stable until a pressure of 3.95 GPa. Above this pressure, a new polymorph phase is formed, which remains stable until 9 GPa. The present study does not consider this change to the new polymorphic state, so the range of pressures investigated is up to 3.95 GPa.

The results of MP and NPT-MD calculations are summarized in Table 1 and compared with experimental data in Figure 2. At  $P = 0$  the relative differences between the predicted and the experimental values are very small. By considering as the reference for comparison the results determined by Olinger et al. [27], the percentage errors for lattice dimensions  $a$ ,  $b$ , and  $c$  are 0.64%, 0.47%, and  $-1.01\%$  for MP results and 1.52%, 1.73%, and 0.12% for the MD-NPT data. The increase of pressure from 0 to 3.95 GPa does not significantly change the differences between the predicted and the experimental sets of values. For example, at the largest pressure considered here (3.95 GPa), the corresponding percent deviations are 0.66%, 2.23%, and 0.29% for the MP values and 0.91%, 2.60%, and 0.54% for the MD-NPT data. It appears that there is a slight increase of the deviation from the experimental data with pressure for the  $b$  lattice dimensions only; the relative differences between experiment and predictions of the other lattice

**Table 1. Lattice Parameters Obtained in Crystal Packing and Molecular Dynamics Calculations for the  $\alpha$ -RDX Crystal as a Function of Pressure at T = 298 K<sup>a</sup>**

Pressure (GPa)	Molecular Packing				NPT-MD			
	Lattice Lengths			Unit Cell Volume ( $\text{\AA}^3$ )	Lattice Lengths			Unit Cell Volume ( $\text{\AA}^3$ )
	<i>a</i> ( $\text{\AA}$ )	<i>b</i> ( $\text{\AA}$ )	<i>c</i> ( $\text{\AA}$ )		<i>a</i> ( $\text{\AA}$ )	<i>b</i> ( $\text{\AA}$ )	<i>c</i> ( $\text{\AA}$ )	
Exp <sup>b</sup>	13.182	11.574	10.709	1633.856	—	—	—	—
Exp <sup>c</sup>	13.202	11.596	10.717	1640.670	—	—	—	—
0.00	13.2863	11.6510	10.6086	1642.197	13.4024	11.7974	10.7305	1696.629
0.50	13.1934	11.5410	10.4855	1596.575	13.2771	11.6513	10.5692	1635.074
0.73	13.1581	11.4986	10.4395	1579.493	13.2334	11.5961	10.5109	1612.963
1.75	13.0005	11.3617	10.2797	1518.392	13.0537	11.4283	10.3277	1540.740
2.75	12.8624	11.2696	10.1669	1473.734	12.9042	11.3204	10.2010	1490.185
3.36	12.8027	11.2189	10.1090	1451.978	12.8399	11.2638	10.1361	1465.962
3.95	12.7535	11.1742	10.0589	1433.495	12.7848	11.2139	10.0838	1445.703

<sup>a</sup> The experimental values indicated correspond to T = 298 K and atmospheric pressure.

<sup>b</sup> Neutron-diffraction values from Choi and Prince [26].

<sup>c</sup> X-ray diffraction values from Olinger et al. [27].

dimensions remain practically unchanged. The corresponding parameters of the quadratic fits of the predicted lattice parameters and volume as function of pressure are given in Table 2. An important finding is that lattice dimensions predicted in MP calculations are very close to the experimental data. This is notable since MP calculations require significantly less computational time than the corresponding NPT-MD calculations.

The normalized dependence of the unit cell volume on pressure is shown in Figure 2(b). The volume compressibility predicted in from NPT-MD simulations is very close to that seen experimentally. The calculated ratio  $V/V_0$  obtained in MD simulations at 3.95 GPa is 0.852, while the corresponding experimental value [27] is 0.846. At this pressure, the predicted MP ratio is slightly larger, with a value of 0.873.

The dependence of the NPT-MD unit cell volume on pressure was determined by fitting the calculated values to the Murnaghan equation [28]:

**Table 2. Coefficients of the Quadratic Fits of the Form  $a_0+a_1P+a_2P^2$  for RDX, HMX, and HNIW and of the Cubic Fit of the Form  $a_0(1+a_1P+a_2P^2+a_3P^3)$  for PETN of the Lattice Constants and Unit Cell Volume as Function of Pressure (GPa) Using Results From the NPT-MD Calculations.<sup>a</sup> The Calculated Bulk Modulus ( $B_0$ ), its Pressure Derivative at Zero Pressure ( $B_0'$ ), and Zero Volume Coefficient Using Equation (3) Are Indicated Together With the Corresponding Experimental Values Where Available**

System	$a_0$	$a_1$	$a_2$	$V_{\text{ofit}}$ ( $\text{\AA}^3$ )	$B_0$ (GPa)	$B_0'$	$B_{0\text{exp}}$ (GPa)	$B'_{0\text{exp}}$	
<b>RDX</b>									
$a$	13.3964	-0.23490.0201	0.0201	—	—	—	—	—	
$b$	11.7786	-0.24620.0269	0.0269	—	—	—	—	—	
$c$	10.7103	-0.2699	0.0289	—	—	—	—	—	
$V$	1689.604 7	-104.9649	11.1950	1639.62	12.93	6.77	13.0 <sup>a</sup>	6.6 <sup>a</sup>	
<b><math>\beta</math>-HMX (P2<sub>1</sub>/c setting)</b>									
$a$	6.5746	-0.0947	0.0061	—	—	—	—	—	
$b$	11.0206	-0.1488	0.0091	—	—	—	—	—	
$c$	9.0416	-0.1252	0.0078	—	—	—	—	—	
$V$	531.1252	-22.72731	1.5919	534.88	14.53	9.57	13.5 <sup>a</sup>	9.3 <sup>a</sup>	
<b><math>\beta</math>-HMX (P2<sub>1</sub>/n setting)</b>									
$a$	6.5069	-0.0803	0.0046	—	—	—	—	—	
$b$	10.9275	-0.1317	0.0070	—	—	—	—	—	
$c$	7.3745	-0.1061	0.0075	—	—	—	—	—	
$V$	516.3269	-19.4548	1.2220	519.79	16.86	9.50	—	—	
<b><math>\epsilon</math>-HNIW</b>									
$a$	8.8956	-0.1215	0.0113	—	—	—	—	—	
$b$	12.5774	-0.2564	0.0288	—	—	—	—	—	
$c$	13.5481	-0.2475	0.0257	—	—	—	—	—	
$V$	1461.6076	-75.4732	8.3433	1463.99 1465.49	15.58 14.67	9.37 9.93	—	—	
<b>PETN</b>									
	$a_0$	$a_1$	$a_2$	$a_3$	$V_{\text{ofit}}$ ( $\text{\AA}^3$ )	$B_0$ (GPa)	$B_0'$	$B_{0\text{exp}}$ (GPa)	$B'_{0\text{exp}}$
$a$ (md)	9.3348	$1.552 \times 10^{-2}$	$1.863 \times 10^{-3}$	$-0.920 \times 10^{-4}$	—	—	—	—	—
$a$ (exp) <sup>b</sup>	9.3830	$-2.052 \times 10^{-2}$	$2.230 \times 10^{-3}$	$-1.041 \times 10^{-4}$	—	—	—	—	—
$c$ (md)	6.6500	$-1.921 \times 10^{-2}$	$2.101 \times 10^{-3}$	$-1.021 \times 10^{-4}$	—	—	—	—	—
$c$ (exp) <sup>b</sup>	6.7150	$-2.832 \times 10^{-2}$	$3.295 \times 10^{-3}$	$-1.458 \times 10^{-4}$	—	—	—	—	—
$V$ (md)	578.7628	$-4.8934 \times 10^{-2}$	$5.839 \times 10^{-3}$	$-2.880 \times 10^{-4}$	582.49	14.09	10.39	9.9 <sup>c</sup>	11.0 <sup>c</sup>

<sup>a</sup> The calculated bulk modulus ( $B_0$ ), its pressure derivative at zero pressure ( $B_0'$ ), and zero volume coefficient using equation (3) are indicated together with the corresponding experimental values where available.

<sup>b</sup> Data from Olinger et al. [27].

<sup>c</sup> Data from Olinger et al. [32].

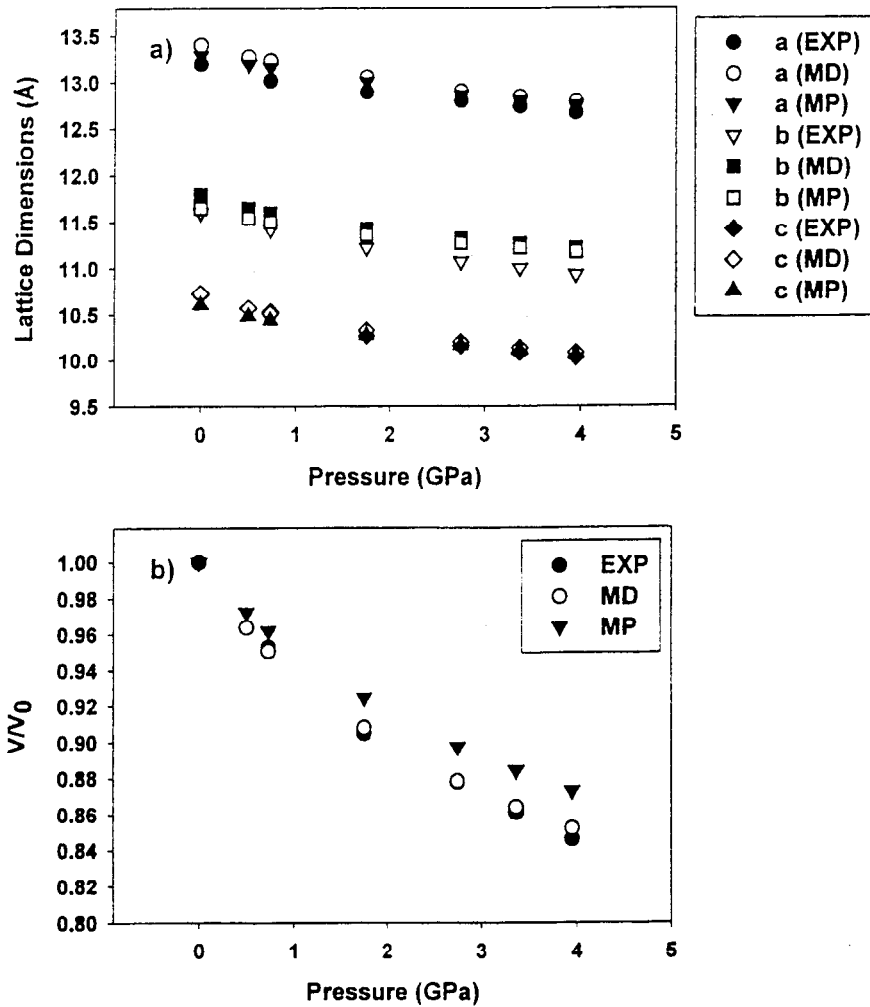


**Figure 2. Comparison of the Crystallographic Parameters Obtained in MP and NPT-MD Simulations for the  $\alpha$ -RDX Crystal With the Experimental Results. Dependence of (a) Lattice Dimensions and (b) Volume Compression  $V/V_0$  on the External Pressure.**

$$P = \frac{B_0}{B_0'} \left[ \left( \frac{V_0}{V} \right)^{B_0'} - 1 \right]. \quad (3)$$

In this equation,  $V$  is the volume at pressure  $P$ ,  $V_0$  is the fitted volume at  $P = 0$ ,  $B_0$  is the bulk modulus, and  $B_0' = dB_0/dP$ . The best-fit parameters are given in Table 2. The predicted bulk modulus and its pressure derivative are very close to the corresponding experimental values with relative percentage errors of  $-0.5\%$  and  $2.5\%$ , respectively.

**4.2 HMX Crystal.** Crystalline HMX can exist in four polymorphic phases, known as the  $\alpha$ ,  $\beta$ ,  $\gamma$ , and  $\delta$  forms [3]. The stable form at room temperature is  $\beta$ -HMX. It has a monoclinic structure with  $P2_1/n$  symmetry [29] or alternatively  $P2_1/c$ , [30, 31] with  $Z = 2$  molecules per unit cell. Olinger et al. [27] have investigated the structure of the  $\beta$ -phase within  $P2_1/c$  symmetry settings for pressures up to 7.47 GPa and have shown that, for this entire pressure range, the crystal remains stable. In a previous study [3], the thermal expansion properties of the crystallographic  $\beta$ -phase described within  $P2_1/n$  symmetry was investigated. In order to reconcile the two possible settings of the same phase (i.e., with  $P2_1/n$  or  $P2_1/c$  symmetries), the MP and NPT-MD results are presented for both of these symmetries. The corresponding results are presented in Table 3 and compared to the experimental data in Figure 3. The predicted lattice dimensions and unit cell volume in NPT-MD simulations at 298 K and zero pressure starting with the structure with  $P2_1/n$  symmetry are in extremely good agreement with the corresponding experimental data. The percent errors for lattice dimensions  $a$ ,  $b$ ,  $c$ , and unit cell volume are  $-19\%$ ,  $-0.72\%$ ,  $0.64\%$ , and  $0.66\%$ , respectively. The corresponding MP results indicate a similarly good agreement with a maximum deviation of  $-1.79\%$  for the lattice dimension  $b$  and  $-1.48\%$  for the unit cell volume. Similar NPT-MD simulations using the structure with the  $P2_1/c$  symmetry give results that are slightly less accurate: the maximum deviations are  $4.1\%$  for lattice dimension  $c$  and  $3.18\%$  for the unit cell volume.

The effect of increasing the pressure on lattice dimensions and volume is also shown in Figure 3 and Table 3. The results in the upper frame correspond to those obtained from NPT-MD and MP calculations starting with the structure with the  $P2_1/c$  symmetry. The predicted dimensions  $a$  and  $c$  remain very close to the experimental values, while the  $b$  dimension deviates slightly with the increase of pressure. In Figure 3(b), the variation of the relative volume  $V/V_0$  is compared for both  $P2_1/c$  and  $P2_1/n$  symmetries with corresponding experimental results [27]. The NPT-MD predictions for either space group are in closer agreement to the experimental result than the MP calculations. For example, the curve  $V/V_0$  for  $P2_1/c$  is extremely close to the experimental values with a deviation at 7.47 GPa of  $0.18\%$ , while, for the  $P2_1/n$  setting, the difference of  $1.45\%$ . Also, as seen in the RDX calculations, MP predictions for both lattice dimensions and lattice volume of  $\beta$ -HMX crystal are close but slightly

**Table 3. Lattice Parameters Obtained in Crystal Packing and Molecular Dynamics Calculations for the  $\beta$ -HMX Crystal as a Function of Pressure at T = 298 K**

Pressure (GPa)	Molecular Packing					NPT-MD				
	Lattice Parameters				Unit Cell Volume ( $\text{\AA}^3$ )	Lattice Parameters				Unit Cell Volume ( $\text{\AA}^3$ )
	$a$ ( $\text{\AA}$ )	$b$ ( $\text{\AA}$ )	$c$ ( $\text{\AA}$ )	$\beta$ ( $^\circ$ )		$a$ ( $\text{\AA}$ )	$b$ ( $\text{\AA}$ )	$c$ ( $\text{\AA}$ )	$\beta$ ( $^\circ$ )	
<b><math>P2_1/n</math> Setting</b>										
Exp <sup>a</sup>	6.5347	11.0296	7.3549	102.69	517.156	—	—	—	—	—
0.00	6.4757	10.8321	7.3729	99.91	509.456	6.5219	10.9499	7.4030	100.03	520.583
0.50	6.4295	10.7636	7.3020	99.82	497.925	6.4663	10.8614	7.3210	99.90	506.542
1.00	6.3924	10.7062	7.2503	99.80	488.955	6.4219	10.7872	7.2590	99.86	495.417
1.61	6.3548	10.6469	7.2013	99.82	480.092	6.3802	10.7203	7.2022	99.88	485.333
2.47	6.3105	10.5748	7.1496	99.88	470.036	6.3292	10.6364	7.1470	99.92	473.916
3.24	6.2768	10.5189	7.1135	99.94	462.623	6.2945	10.5743	7.1075	99.99	465.917
4.03	6.2467	10.4682	7.0828	100.00	456.116	6.2628	10.5177	7.0794	100.07	459.167
4.82	6.2197	10.4228	7.0566	100.07	450.409	6.2328	10.4633	7.0525	100.11	452.792
5.42	6.2009	10.3905	7.0394	100.12	446.498	6.2138	10.4321	7.0319	100.16	448.667
6.31	6.1756	10.3471	7.0165	100.19	441.278	6.1859	10.3827	7.0110	100.23	443.125
6.74	6.1640	10.3274	7.0065	100.22	438.938	6.1744	10.3592	7.0016	100.26	440.708
7.47	6.1457	10.2954	6.9908	100.28	435.224	6.1549	10.3242	6.9866	100.32	436.792
<b><math>P2_1/c</math> Setting</b>										
Exp <sup>b</sup>	6.540	11.050	8.700	124.30	519.387	—	—	—	—	—
Exp <sup>c</sup>	6.533	11.030	8.699	124.45	516.906	—	—	—	—	—
0.00	6.5392	10.9220	9.0213	125.65	523.593	6.5922	11.0441	9.0586	125.65	535.916
0.50	6.4846	10.8484	8.9521	125.88	510.285	6.5243	10.9433	8.9771	125.93	518.958
1.00	6.4423	10.7870	8.8946	125.97	500.199	6.4736	10.8647	8.9136	126.05	506.833
1.61	6.4002	10.7236	8.8349	126.02	490.397	6.4278	10.7904	8.8481	126.12	495.708
2.47	6.3519	10.6480	8.7652	126.03	479.455	6.3739	10.7008	8.7750	126.12	483.458
3.24	6.3159	10.5900	8.7128	125.99	471.492	6.3342	10.6362	8.7204	126.08	474.791
4.03	6.2835	10.5375	8.6658	125.95	464.514	6.2989	10.5786	8.6699	126.01	467.291
4.82	6.2551	10.4906	8.6240	125.89	458.448	6.2678	10.5281	8.6264	125.94	460.833
5.42	6.2352	10.4580	8.5955	125.85	454.331	6.2468	10.4892	8.5991	125.89	456.416
6.31	6.2086	10.4128	8.5567	125.78	448.785	6.2187	10.4402	8.5604	125.83	450.583
6.74	6.1966	10.3929	8.5389	125.75	446.315	6.2058	10.4203	8.5421	125.79	448.042
7.47	6.1775	10.3607	8.5108	125.69	442.411	6.1852	10.3844	8.5138	125.73	443.875

<sup>a</sup> Data from Cromer et al. [29].

<sup>b</sup> Data from Kohno et al. [30] and Choi and Boutin [31].

<sup>c</sup> Data from Olinger et al. [27].

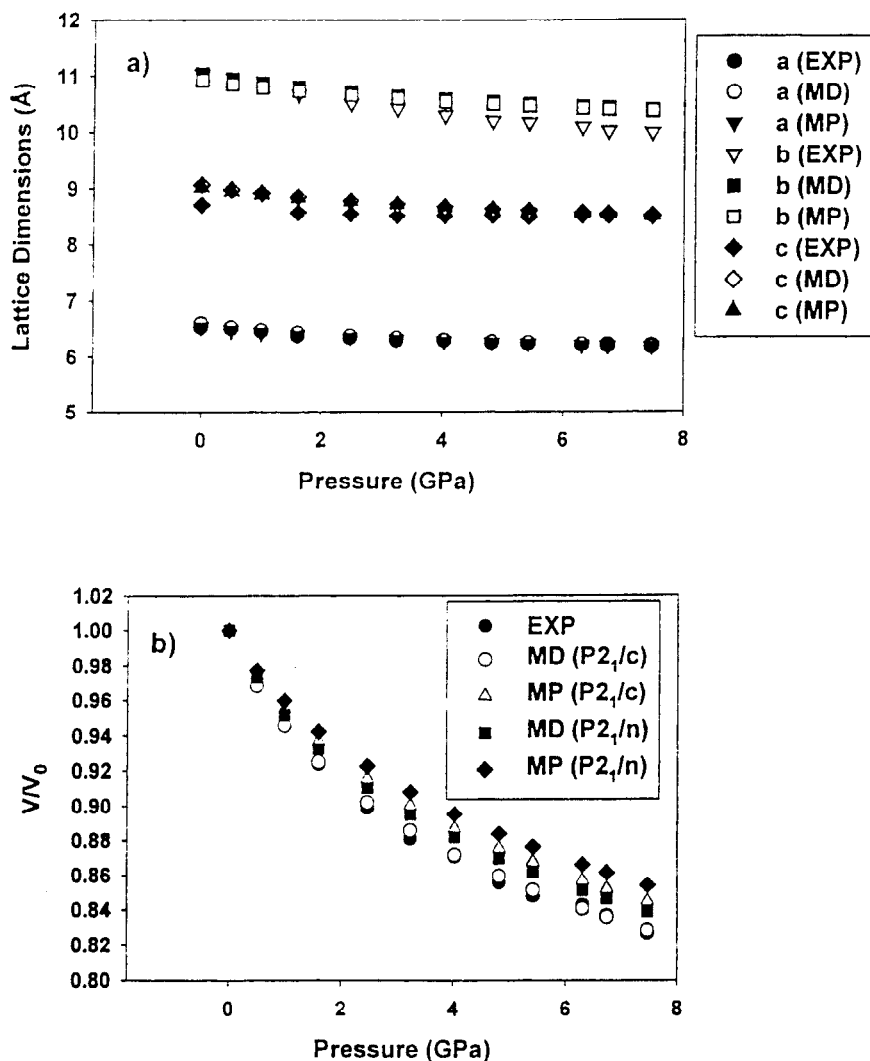


**Figure 3. Comparison of the Crystallographic Parameters Obtained in MP and NPT-MD Simulations for the  $\beta$ -HMX Crystal With the Experimental Results. The Variations of Lattice Dimensions Indicated in the Top Panel (a) Correspond to the Structure With  $P2_1/c$  Symmetry Where Experimental Data Are Available. The Lower Panel (b) Indicates the Variations of the Relative Volume as a Function of Pressure for Both  $P2_1/c$  and  $P2_1/n$  Symmetries Together With the Corresponding Experimental Results.**

less accurate than are the corresponding NPT-MD results. This result is expected because MP calculations do not include the thermal effects considered in NPT-MD simulations. Consequently, the predicted lattices are less compressible than would be expected in a simulation that correctly incorporates thermal effects.

The bulk modulus and pressure derivative calculated using the results from Table 3 and equation (3) are given in Table 2. The results are in reasonable agreement with experimental values, though the variation from experiment is larger for HMX than the RDX results. The  $P2_1/c$  results are closer to experiment than those determined from the  $P2_1/n$  results.

**4.3 HNIW Crystal.** HNIW, a polycyclic nitramine, has been characterized as “the densest and most energetic explosive known” [33]. It exists in at least five polymorphic states, four of which are stable at ambient conditions and have been resolved ( $\alpha$ -hydrate,  $\epsilon$ ,  $\beta$ , and  $\gamma$ ) by x-ray crystallography [34]. The molecular structure of these polymorphs appears to be that of two bridged RDX molecules and is similar to that shown in Figure 1(c) for the  $\epsilon$ -phase. The main differences between the configurations of the different polymorphs are in the orientation of the nitrogroups relative to the ring. The  $\epsilon$  polymorph that is considered in this work is the most stable phase at room temperature [2]. It crystallizes in the  $P2_1/n$  space group and has  $Z = 4$  molecules per unit cell [35].

The calculated lattice dimensions at different pressures for this crystal are given in Table 4 and a visual comparison of the experimental data of Pinkerton [35] is given in Figure 4. The lattice dimensions predicted by MD-NPT and MP simulations are in very good agreement with the experimental values. For example, at the highest pressure considered experimentally (2.5 GPa), the deviations from experiment are 1.47%, 1.73%, and 2.17% for the  $a$ ,  $b$ , and  $c$  lattice dimensions, respectively. Also, for this pressure, the calculated volumetric compression shown in Figure 4(b) is 0.90, while the corresponding experimental value is 0.88. Using the variation of the unit cell volume given in Table 4 with pressure and equation (3), a bulk modulus  $B_0 = 15.58$  GPa and a pressure derivative  $B_0' = 9.37$  have been determined. However, no experimental values were found against which comparison could be made of these calculated values.

**4.4 PETN Crystal.** The final system chosen for assessment of the interaction potential is the non-nitramine explosive PETN. This system could be considered a more difficult test than the preceding systems, since the molecular conformation (see Figure 1[d]) is much more floppy

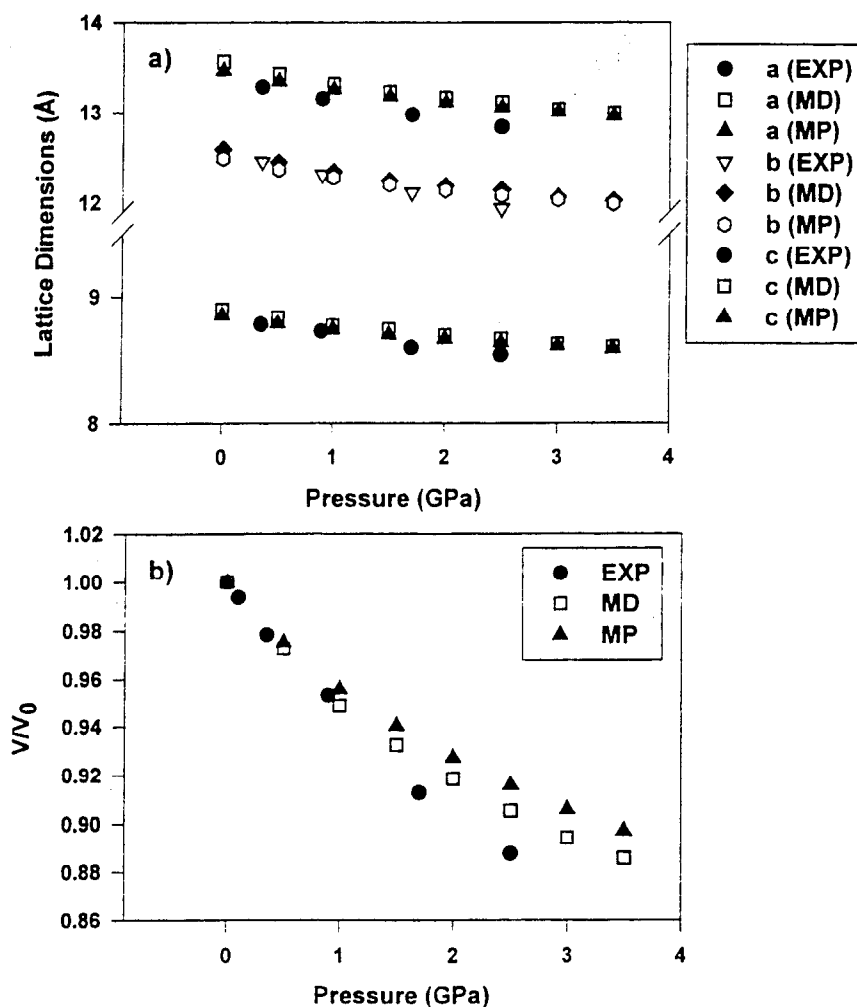


**Figure 4. Comparison of the Crystallographic Lattice Dimensions Obtained in MP and NPT-MD Simulations for the  $\epsilon$ -HNIW Crystal With the Experimental Results. Dependence of (a) Lattice Dimensions and (b) Volume Compression  $V/V_0$  on the External Pressure.**

than in the previous three systems. This characteristic suggests that the rigid-body approximation assumed in the simulations might be inadequate. Consequently, it is expected that predictions of crystallographic parameters for this type of crystal within the constraints of these simulations will be less accurate than those obtained previously, particularly for the higher pressure regime.

The experimental investigations have shown that PETN can exist in two different phases: a tetragonal phase, also called form i [37] and an orthorhombic phase, known as form ii [38]. Both

**Table 4. Lattice Parameters Obtained in Crystal Packing and Molecular Dynamics Calculations for the  $\epsilon$ -HNIW Crystal as a Function of Pressure at T = 298 K**

Pressure (GPa)	Molecular Packing				NPT-MD			
	Lattice Lengths			Unit Cell Volume ( $\text{\AA}^3$ )	Lattice Lengths			Unit Cell Volume ( $\text{\AA}^3$ )
	$a$ ( $\text{\AA}$ )	$b$ ( $\text{\AA}$ )	$c$ ( $\text{\AA}$ )		$a$ ( $\text{\AA}$ )	$b$ ( $\text{\AA}$ )	$c$ ( $\text{\AA}$ )	
Exp. <sup>a</sup>	8.8278	12.5166	13.3499	1412.483	—	—	—	—
Exp. <sup>b</sup>	8.8847	12.6210	13.4310	1439.000	—	—	—	—
0.00	8.8550	12.4897	13.4624	1437.349	8.8998	12.5916	13.5600	1464.750
0.50	8.7915	12.3701	13.3448	1401.346	8.8375	12.4457	13.4238	1424.500
1.00	8.7429	12.2784	13.2530	1373.862	8.7727	12.3399	13.3132	1389.833
1.50	8.6696	12.1403	13.1119	1351.604	8.7440	12.2432	13.2245	1365.917
2.00	8.6696	12.1403	13.1119	1332.776	8.6981	12.1857	13.1631	1345.417
2.50	8.6403	12.0851	13.0548	1316.499	8.6699	12.14465	13.1128	1326.120
3.00	8.6143	12.0361	13.0039	1302.117	8.6303	12.06299	13.0326	1309.750
3.50	8.5911	11.9920	12.9578	1289.259	8.6066	12.02246	12.9882	1287.333

<sup>a</sup> Data from Gilardi [35].

<sup>b</sup> Data obtained from Pinkerton [36] by extrapolation to P = 0.

previous experimental results [39] and theoretical values [5] indicate that the tetragonal phase is the most stable. Therefore, in this study, the phase that crystallizes in space group  $\overline{P4}21c$  and has Z = 2 molecules per unit cell (form i) is analyzed. The results of our MP and NPT-MD calculations are given in Table 5 and shown in Figure 5.

The isothermal linear and volume compression of tetragonal PETN has been previously investigated by Olinger et al. [32] for pressures up to 10 GPa using an x-ray diffraction technique. The pressure dependence of the experimental lattice dimensions and unit cell volume as represented in Figure 5 were fitted using a cubic polynomial in pressure powers given in Table 2 [32]. In the same table, the corresponding best-fit parameters obtained are given based on predicted NPT-MD data given in Table 5. The two sets of fitted parameters have similar values, indicating an acceptable agreement between the experimental and predicted lattice dimensions. A more direct comparison is given in Figure 5(a), where both MD and MP lattice dimensions are represented together with experimental values. In the region of low pressure (<4 GPa), the agreement is very good with relative errors of  $-0.35\%$  and  $-0.67\%$  for the

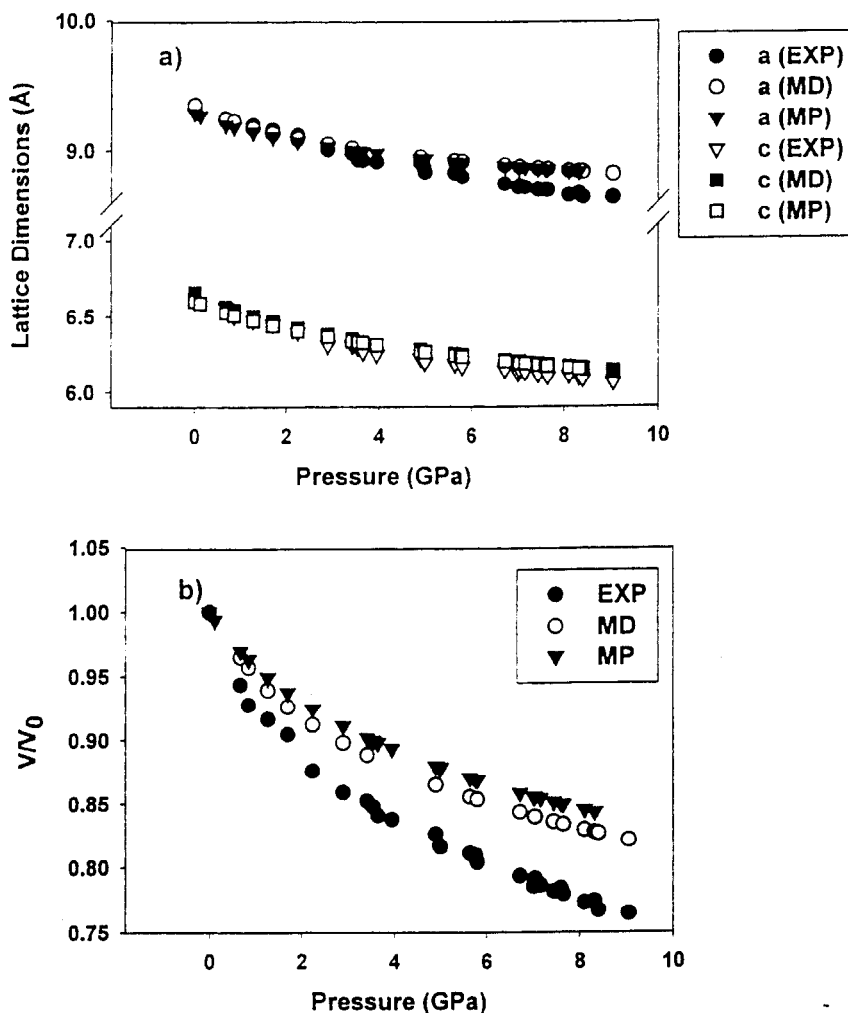


**Figure 5. Comparison of the Crystallographic Parameters Obtained in MP and NPT-MD Simulations for Tetragonal Phase of PETN Crystal With the Experimental Results. Dependence of (a) Lattice Dimensions and (b) Volume Compression  $V/V_0$  on the External Pressure.**

$a$  and  $c$  lattice dimensions and  $-1.44\%$  for the unit cell volume. In addition, as indicated in Table 5, the lattice dimensions  $a$  and  $b$  remain equal (within the errors of simulation), while the cell angles (not shown) remain approximately  $90.0^\circ$  in agreement with the tetragonal symmetry of the lattice. By increasing the pressure from 0 to 9 GPa, it can be seen in Figure 5 that the predicted lattice dimensions are very close to the experimental values up to about 6 GPa. For this pressure, the relative errors are 1.33% and 1.25% for the  $a$  and  $c$  dimensions. Above 6 GPa, the deviations of the predicted values from the experiment increase more rapidly, reaching values of  $-2.08\%$

**Table 5. Lattice Parameters Obtained in Crystal Packing and Molecular Dynamics Calculations for the PETN Crystal as a Function of Pressure at T = 298 K**

Pressure (GPa)	Molecular Packing				NPT-MD			
	Lattice Lengths			Unit Cell Volume	Lattice Lengths			Unit Cell Volume
	<i>a</i> (Å)	<i>b</i> (Å)	<i>c</i> (Å)	(Å <sup>3</sup> )	<i>a</i> (Å)	<i>b</i> (Å)	<i>c</i> (Å)	(Å <sup>3</sup> )
Exp. <sup>a</sup>	9.3776	9.3776	6.7075	589.853	—	—	—	—
Exp. <sup>b</sup>	9.3860	9.3860	6.7150	591.571	—	—	—	—
0.00	9.2843	9.2841	6.5995	568.853	9.3467	9.3410	6.6546	580.996
0.68	9.1950	9.1950	6.5214	551.371	9.2411	9.2418	6.5609	560.414
0.86	9.1762	9.1760	6.5043	547.667	9.2185	9.2202	6.5404	555.972
1.28	9.1371	9.1370	6.4682	540.002	9.1661	9.1659	6.4967	545.833
1.71	9.1028	9.1025	6.4358	533.259	9.1275	9.1286	6.4603	538.278
2.25	9.0654	9.0652	6.3997	525.925	9.0851	9.0880	6.4209	530.139
2.90	9.0269	9.0267	6.3616	518.363	9.0454	9.0450	6.3789	521.899
3.42	8.9998	8.9997	6.3342	513.042	9.0168	9.0162	6.3499	516.250
4.90	8.9359	8.9358	6.2674	500.448	8.9476	8.9476	6.2791	502.714
5.64	8.9093	8.9091	6.2384	495.166	8.9197	8.9193	6.2495	497.199
5.80	8.9039	8.9036	6.2325	494.092	8.9134	8.9132	6.2423	495.934
6.73	8.8746	8.8743	6.2000	488.286	8.8835	8.8835	6.2089	489.994
7.05	8.8618	8.8617	6.1855	485.751	8.8722	8.8724	6.1983	487.918
7.45	8.8540	8.8538	6.1767	484.201	8.8609	8.8608	6.1843	485.559
7.65	8.8486	8.8484	6.1705	483.125	8.8549	8.8554	6.1780	484.438
8.11	8.8365	8.8364	6.1566	480.725	8.8422	8.8432	6.1639	481.982
8.32	8.8312	8.8311	6.1504	479.665	8.8376	8.8373	6.1571	480.869
8.40	—	—	—	—	8.8355	8.8354	6.1543	480.441
9.04	—	—	—	—	8.8195	8.8192	6.1357	477.250

<sup>a</sup> Data from Trotter [37].

<sup>b</sup> Data from Olinger et al. [32].

and 1.26% for the *a* and *c* dimensions, respectively, at P = 8.84 GPa. This trend is accentuated in the variation of the relative volume  $V/V_0$ , where the deviation at 5 GPa is about 4.6%, while, at 8.84 GPa, the deviation reaches a value of 7.8%. The lower compressibility of the theoretical model is also reflected in the bulk modulus. The predicted bulk modulus using equation (3) and the data in Table 5 is 14.0 GPa, while the experimental value is 9.9 GPa [32]. Thus, it is evident that the assumption of rigid molecules in these molecular simulations is invalid for pressures above 5 GPa.

Changes in volume with pressure upon uniaxial compression in either dimension have also been explored using this model. This investigation is accomplished using the pressure dependencies of the individual lattice parameters determined in Table 2, which are assumed to remain valid in the case of uniaxial compression. The results presented in Figure 6 clearly indicate that for a given applied external pressure the variation of the volume is larger in the case of compression along *c*-axis than in the case of *a*-axis. This result indicates a strong sensitivity of the volume change with the type of compression applied and is in agreement with the findings reported by Kunz [40] based on ab initio periodic Hartree-Fock calculations.

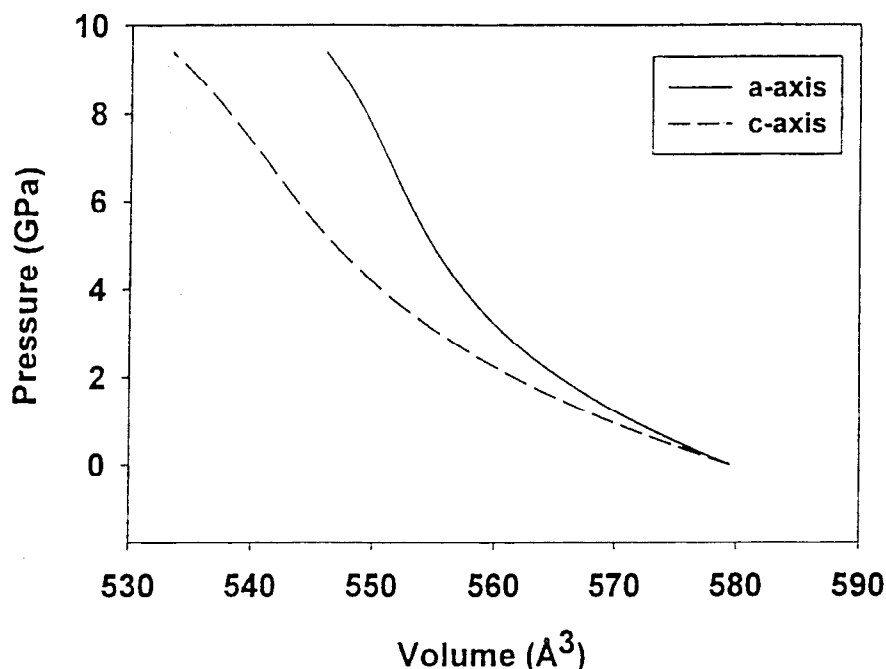


**Figure 6. The Pressure-Volume Dependence for PETN in the Case of Uniaxial Compression Along *a*-Axis and *c*-Axis, Respectively. The Calculated Curves Have Been Determined Using the Pressure Coefficients Indicated in Table 2.**

Considering the ensemble of results presented in this work, it appears that the rigid-molecule model can be used in connection with the present intermolecular potential within a carefully considered range of pressures. Depending on the type of molecular structure (i.e., more floppy as PETN, or more rigid as [poly]cyclic nitramines RDX, HMX, and HNIW), the range of pressures in which realistic predictions can be made varies from about 5 GPa in the case of PETN to more than 7.5 GPa for HMX. The main effect of the initial compression of these

crystals is represented by reduction of the intermolecular distances. Such an effect can be seen in Figure 7, where the RDFs of the COM-COM pairs for all molecules in the MD simulation box are represented. The main changes in the RDF distributions are the shifts of the peaks toward smaller distance values with increasing pressure, indicating the compression of these materials. In addition, there is a continuous decrease of the amplitude of molecular oscillations around the equilibrium positions reflected by additional resolved peaks, particularly for the HMX and HNIW structures.

## 5. Conclusions

The hydrostatic compression effects have been investigated on some important energetic materials RDX, HMX, HNIW, and PETN through crystal packing and isothermal-isobaric molecular dynamics simulations. The potential used in these calculations was previously developed for RDX and shown to be transferable to 30 nitramine crystals [4] and to 51 other non-nitramine crystals [5] consisting of molecules that contained functional groups associated with energetic materials. These systems include different types of nitroalkanes, nitroaromatics, nitrocubanes, polynitroadamantes, hydroxy-nitroderivatives, nitrobenzotriazoles, and nitrate esters.

The tests of this potential indicate that the predictions of the crystallographic parameters for RDX, HMX, and HNIW are very good with lattice dimension errors below 2.2% for RDX, 4.1% for HMX, and 2.17% for HNIW. Moreover, this potential is able to predict both the changes of the crystallographic structures with pressure and the bulk moduli and pressure derivatives. For RDX, the predicted bulk modulus at zero pressure is  $B_0 = 12.93$  GPa, while the experimental value is  $B_{0\text{exp}} = 13.0$  GPa. Similarly, for HMX  $B_0 = 14.64$  GPa vs. an experimental value  $B_{0\text{exp}} = 13.5$  GPa.

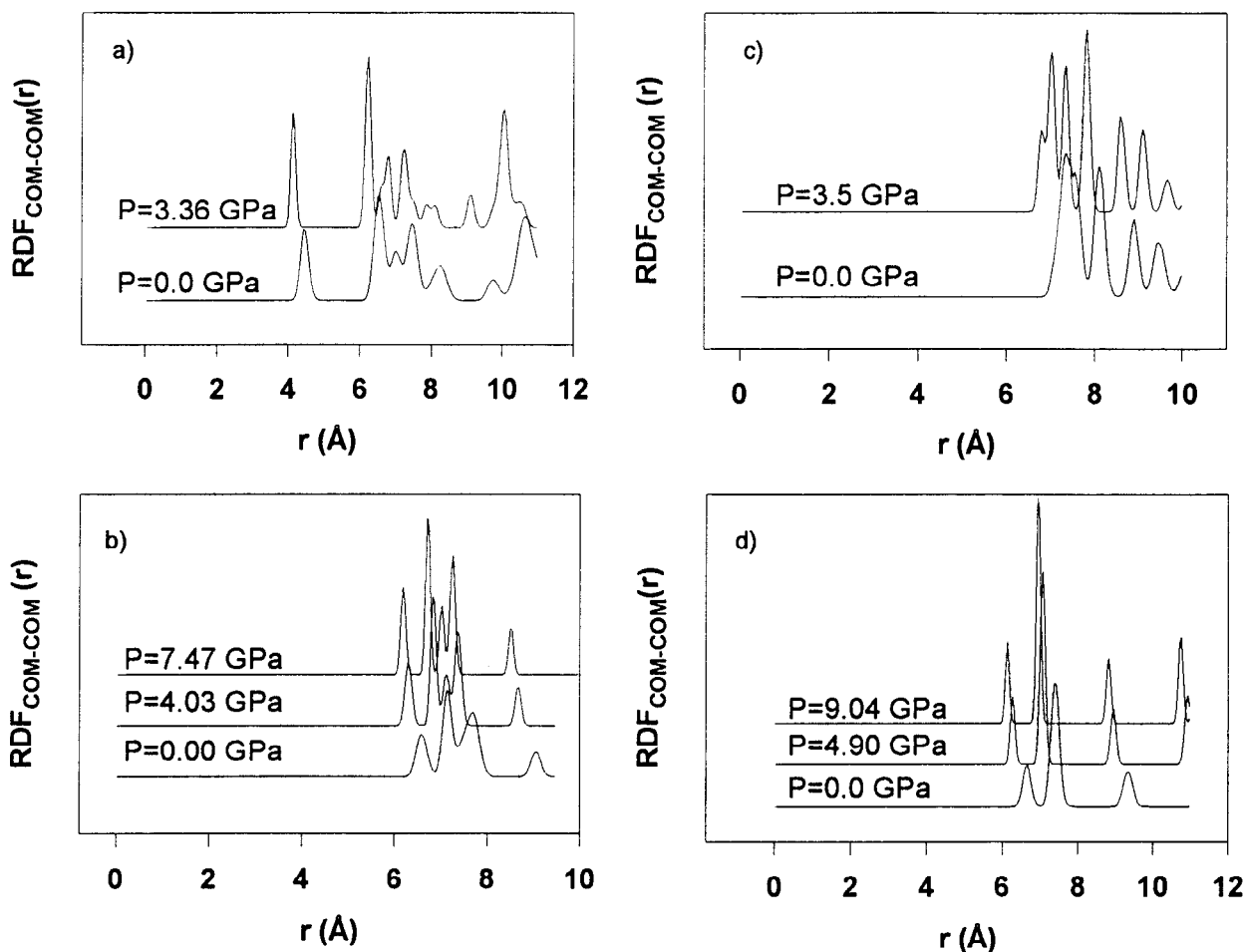


**Figure 7. Radial Distribution Functions for COM-COM Pairs as Function of Pressure for (a)  $\alpha$ -RDX, (b)  $\beta$ -HMX, (c)  $\epsilon$ -HNIW; and (d) PETN (Tetragonal Phase).**

Another finding of the present work is that molecular-packing calculations give crystallographic parameters that are very close to those determined in NPT-MD simulations but at a fraction of cost in the computing time. This result indicates the utility of MP calculations not only for equilibrium crystallographic structures but also when the compression effects are of interest.

In the case of crystals with floppy molecules such as PETN, the range of pressure over which the present model can make accurate predictions is more limited, in this case, to about 5 GPa.

This result does not represent a limitation of the potential parameters involved but rather indicates that the rigid molecular model used fails to be valid for such systems.

The success of the present potential energy parameters in describing not only the ambient equilibrium structures of different crystals with functional groups associated with explosives but also the effects of external stimuli, such as pressure and temperature, provides significant incentive to further develop this model by incorporating the intramolecular degree of freedom. This will be done in future work.

INTENTIONALLY LEFT BLANK.

## 6. References

1. Sorescu, D. C., B. M. Rice, and D. L. Thompson. *Journal of Physical Chemistry B*. Vol. 101, p. 798, 1997.
2. Sorescu, D. C., B. M. Rice, and D. L. Thompson. *Journal of Physical Chemistry B*. Vol. 102, p. 948, 1998.
3. Sorescu, D. C., B. M. Rice, and D. L. Thompson. *Journal of Physical Chemistry B*. Vol. 102, p. 6692, 1998.
4. Sorescu, D. C., B. M. Rice, and D. L. Thompson. *Journal of Physical Chemistry A*. Vol. 102, p. 8386, 1998.
5. Sorescu, D. C., B. M. Rice, and D. L. Thompson. *Journal of Physical Chemistry A*. Vol. 103, p. 989, 1998.
6. Russell, T. P., P. J. Miller, G. J. Piermarini, S. Block, R. Gilardi, and C. George. AD-CO48 931 (92-0134), CPIA Abstract No. 92, 0149, ADD604 42. C-D, p.155, Chemical Propulsion Information Agency, Columbia, MD, April 1991.
7. McCrone, W. C. *Physics and Chemistry of the Organic Solid State*. D. Fox, M. M. Labes, and A. Weissberger (editors), vol. 2, pp. 726–766, New York, NY: Wiley, 1965.
8. Breneman, C. M., and K. B. Wiberg. *Journal of Computational Chemistry*. Vol. 11, p. 361, 1990.
9. Möller, C. M. S. *Physical Review*. Vol. 46, p. 618, 1934.
10. Hehre, W. J., R. Ditchfield, and J. A. Pople. *Journal of Chemical Physics*. Vol. 56, p. 2257, 1972.
11. Hariharan, P. C., and J. A. Pople. *Theoretica Chimica Acta*. Vol. 28, p. 213, 1973.
12. Gordon, M. S. *Chemical Physics Letters*. Vol. 76, p. 163, 1980.
13. Pastine, D., and R. R. Bernecker. *Journal of Applied Physics*. Vol. 45, p. 4458, 1974.
14. Sewell, T. D. *Journal of Applied Physics*. Vol. 83, p. 4142, 1998.

15. Frisch, M. J., G. W. Trucks, H. B. Schlegel, P. M. W. Gill, B. G. Johnson, M. A. Robb, J. R. Cheeseman, T. Keith, G. A. Paterson, J. A. Montgomery, K. Raghavachari, M. A. Al-Laham, V. G. Zakrzewski, J. V. Ortiz, J. B. Foresman, J. Cioslowski, B. B. Stefanov, A. Nanyakkara, M. Challacombe, C. Y. Peng, P. Y. Ayala, W. Chen, M. W. Wong, J. L. Andres, E. S. Replogle, R. Gomperts, R. L. Martin, D. J. Fox, J. S. Binkley, D. J. Defrees, J. Baker, J. P. Stewart, M. Head-Gordon, C. Gonzales, and J. A. Pople. *Gaussian 94*. Revision C.3, Gaussian, Inc., Pittsburgh, PA, 1995.
16. Hariharan, P. C., and J. A. Pople. *Theoretica Chimica Acta*. Vol. 28, p. 213, 1973.
17. Pertsin, A. J., and A. I. Kitaigorodsky. *The Atom-Atom Potential Method, Applications to Organic Molecular Solids*. Berlin: Springer-Verlag, 1987.
18. Desiraju, G. R. *Crystal Engineering: The Design of Organic Solids*. Amsterdam: Elsevier, 1989.
19. Gibson, K. D., and H. A. Scheraga. *Journal of Physical Chemistry*. Vol. 99, p. 3752, 1995.
20. Gibson, K. D., and H. A. Scheraga. *LMIN: A Program for Crystal Packing*. QCPE No. 664.
21. Busing, W. R., and M. Matsui. *Acta Crystallography*. Vol. A40, p. 532, 1984.
22. Melchionna, S., G. Ciccotti, and B. L. Holian. *Molecular Physics*. Vol. 78, p. 533, 1993.
23. Allen, M. P., and D. J. Tildesley. *Computer Simulation of Liquids*. New York, NY: Oxford University Press, 1989.
24. Fincham, D. *Molecular Simulation*. Vol. 8, p. 165, 1992.
25. McCrone, W. C. *Analytical Chemistry*. Vol. 22, p. 954, 1950.
26. Choi, C. S., and E. Prince. *Acta Crystallography*. Vol. B28, p. 2857, 1972.
27. Olinger, B., B. Roof, and H. Cady. *Symposium International Sur Le Comportement Des Milieux Denses Sous Hautes Pressions Dynamiques*. Paris, France, p. 3, 1978.
28. Murnaghan F. D. *Finite Deformation of an Elastic Solid*, New York, NY: Dover Publications, p.73, 1951.
29. Cromer, D. T., R. R. Ryan, and D. Schiferl. *Journal of Physical Chemistry*. Vol. 89, p. 2315, 1985.
30. Kohno, Y., K. Maekawa, N. Azuma, T. Tsuchioka, T. Hashizume, and A. Imamura. *Kogyo Kayaku*. Vol. 53, p. 227, 1992 (in Japanese).

31. Choi, C. S., and H. P. Boutin. *Acta Crystallography*. Vol. B26, p. 11235, 1970.
32. Olinger, B., P. M. Halleck, and Cady, H. H. *Journal of Chemical Physics*. Vol. 62, p. 4480, 1975.
33. Miller, R. S. "Decomposition, Combustion and Detonation Chemistry of Energetic Materials." *Materials Research Society Symposium Proceedings*, vol. 418, p. 3, T. B. Brill, T. P. Russell, W. C. Tao, and R. B. Wardle (editors), Materials Research Society, Pittsburgh, PA, 1995.
34. Chan, M. L., P. Carpenter, R. Hollins, M. Nadler, A. T. Nielsen, R. Nissan, D. J. Vanderah, R. Yee, and R. D. Gilardi. CPIA Abstract No. X95-07119, AD D606 761, CPIA-PUB-625, p. 17, April 1995.
35. Gilardi, R. D. Personal communication. 1997.
36. Pinkerton, A. Personal communication. 1999.
37. Trotter, J. *Acta Crystallography*. Vol. 16, p. 698, 1963.
38. Cady, H. H., and A. C. Larson. *Acta Crystallography*. Vol. B41, p. 1864, 1975.
39. Blomquist, A. T., and Ryan, J. F., Jr. "Studies Related to the Stability of PETN." OSRD Report NDRC-B-2566, 1944.
40. Kunz, A. B. *Materials Research Society Symposium Proceedings*. Vol. 418, p. 287, 1996.

INTENTIONALLY LEFT BLANK.

<u>NO. OF COPIES</u>	<u>ORGANIZATION</u>	<u>NO. OF COPIES</u>	<u>ORGANIZATION</u>
2	DEFENSE TECHNICAL INFORMATION CENTER DTIC DDA 8725 JOHN J KINGMAN RD STE 0944 FT BELVOIR VA 22060-6218	1	DIRECTOR US ARMY RESEARCH LAB AMSRL DD 2800 POWDER MILL RD ADELPHI MD 20783-1197
1	HQDA DAMO FDT 400 ARMY PENTAGON WASHINGTON DC 20310-0460	1	DIRECTOR US ARMY RESEARCH LAB AMSRL CI AI R (RECORDS MGMT) 2800 POWDER MILL RD ADELPHI MD 20783-1145
1	OSD OUSD(A&T)/ODDDR&E(R) R J TREW THE PENTAGON WASHINGTON DC 20301-7100	3	DIRECTOR US ARMY RESEARCH LAB AMSRL CI LL 2800 POWDER MILL RD ADELPHI MD 20783-1145
1	DPTY CG FOR RDA US ARMY MATERIEL CMD AMCRDA 5001 EISENHOWER AVE ALEXANDRIA VA 22333-0001	1	DIRECTOR US ARMY RESEARCH LAB AMSRL CI AP 2800 POWDER MILL RD ADELPHI MD 20783-1197
1	INST FOR ADVNCD TCHNLGY THE UNIV OF TEXAS AT AUSTIN PO BOX 202797 AUSTIN TX 78720-2797		<u>ABERDEEN PROVING GROUND</u>
1	DARPA B KASPAR 3701 N FAIRFAX DR ARLINGTON VA 22203-1714	4	DIR USARL AMSRL CI LP (BLDG 305)
1	US MILITARY ACADEMY MATH SCI CTR OF EXCELLENCE MADN MATH MAJ HUBER THAYER HALL WEST POINT NY 10996-1786		
1	DIRECTOR US ARMY RESEARCH LAB AMSRL D D R SMITH 2800 POWDER MILL RD ADELPHI MD 20783-1197		

NO. OF  
COPIES

ORGANIZATION

ABERDEEN PROVING GROUND

22 DIR USARL  
AMSRL WM  
B RINGERS  
AMSRL WM BD  
B E FORCH  
W R ANDERSON  
S W BUNTE  
C F CHABALOWSKI  
A COHEN  
R DANIEL  
D DEVYNCK  
R A FIFER  
B E HOMAN  
A J KOTLAR  
K L MCNESBY  
M MCQUAID  
M S MILLER  
A W MIZIOLEK  
J B MORRIS  
R A PESCE-RODRIGUEZ  
B M RICE  
R C SAUSA  
M A SCHROEDER  
J A VANDERHOFF  
AMSRL WM MB  
B FINK

# REPORT DOCUMENTATION PAGE

Form Approved  
OMB No. 0704-0188

Public reporting burden for this collection of information is estimated to average 1 hour per response, including the time for reviewing instructions, searching existing data sources, gathering and maintaining the data needed, and completing and reviewing the collection of information. Send comments regarding this burden estimate or any other aspect of this collection of information, including suggestions for reducing this burden, to Washington Headquarters Services, Directorate for Information Operations and Reports, 1215 Jefferson Davis Highway, Suite 1204, Arlington, VA 22202-4302, and to the Office of Management and Budget, Paperwork Reduction Project(0704-0188), Washington, DC 20503.

1. AGENCY USE ONLY (Leave blank)		2. REPORT DATE <p style="text-align: center;">April 2001</p>	3. REPORT TYPE AND DATES COVERED <p style="text-align: center;">Final, January - June 1999</p>	
4. TITLE AND SUBTITLE Theoretical Studies of the Hydrostatic Compression of RDX, HMX, HNTW, and PETN Crystals			5. FUNDING NUMBERS 622618.H8000	
6. AUTHOR(S) Dan C. Sorescu, <sup>**</sup> Betsy M. Rice, and Donald L. Thompson <sup>*</sup>				
7. PERFORMING ORGANIZATION NAME(S) AND ADDRESS(ES) U.S. Army Research Laboratory ATTN: AMSRL-WM-BD Aberdeen Proving Ground, MD 21005-5066			8. PERFORMING ORGANIZATION REPORT NUMBER ARL-TR-2453	
9. SPONSORING/MONITORING AGENCY NAMES(S) AND ADDRESS(ES) Strategic Environmental Research and Development Program 901 North Stuart Street, Suite 303 Arlington, VA 22203			10. SPONSORING/MONITORING AGENCY REPORT NUMBER	
11. SUPPLEMENTARY NOTES Oklahoma State University, Stillwater, OK 74078 <sup>†</sup> Current mailing address: Department of Chemistry, University of Pittsburgh, Pittsburgh, PA 15260				
12a. DISTRIBUTION/AVAILABILITY STATEMENT Approved for public release; distribution is unlimited.			12b. DISTRIBUTION CODE	
13. ABSTRACT (Maximum 200 words) <p>A previously developed intermolecular potential for nitramines and several other classes of nitrocompound crystals has been used to investigate the behavior of the energetic materials hexahydro-1,3,5-trinitro-1,3,5-s-triazine (RDX), 1,3,5,7-tetranitro-1,3,5,7-tetraazacyclo-octane (HMX), 2,4,6,8,10,12-hexanitrohexaazaisowurtzitane (HNTW), and pentaerythritol tetranitrate (PETN) under hydrostatic compression. Isothermal-isobaric molecular simulations (assuming the rigid-molecule approximation) molecular-packing calculations were used to perform the analyses. In the case of the RDX, HMX, and HNTW crystals, the results indicate that the proposed potential model is able to accurately reproduce the changes in the structural crystallographic parameters as functions of pressure for the entire range of pressures that has been investigated experimentally. In addition, the calculated bulk moduli of RDX and HMX were found to be in good agreement with the corresponding experimental results. In the case of the PETN crystal, the crystallographic parameters have been reproduced with an acceptable accuracy at pressures up to about 5 GPa. The larger deviations from the experimental results at greater pressures indicate the limitations of the rigid-molecule model when applied to floppy molecules. The similarity of the results determined in molecular-packing calculations relative to those from molecular dynamics simulations suggest that the former method can be used as an efficient tool for rapid tests of the crystal structure modification under pressure.</p>				
14. SUBJECT TERMS molecular dynamics, molecular packing, RDX, HMX, HNTW, PETN			15. NUMBER OF PAGES 35	
			16. PRICE CODE	
17. SECURITY CLASSIFICATION OF REPORT UNCLASSIFIED	18. SECURITY CLASSIFICATION OF THIS PAGE UNCLASSIFIED	19. SECURITY CLASSIFICATION OF ABSTRACT UNCLASSIFIED	20. LIMITATION OF ABSTRACT UL	

INTENTIONALLY LEFT BLANK.

**USER EVALUATION SHEET/CHANGE OF ADDRESS**

This Laboratory undertakes a continuing effort to improve the quality of the reports it publishes. Your comments/answers to the items/questions below will aid us in our efforts.

1. ARL Report Number/Author ARL-TR-2453 (POC: Rice) Date of Report April 2001

2. Date Report Received \_\_\_\_\_

3. Does this report satisfy a need? (Comment on purpose, related project, or other area of interest for which the report will be used.) \_\_\_\_\_  
\_\_\_\_\_

4. Specifically, how is the report being used? (Information source, design data, procedure, source of ideas, etc.) \_\_\_\_\_  
\_\_\_\_\_

5. Has the information in this report led to any quantitative savings as far as man-hours or dollars saved, operating costs avoided, or efficiencies achieved, etc? If so, please elaborate. \_\_\_\_\_  
\_\_\_\_\_

6. General Comments. What do you think should be changed to improve future reports? (Indicate changes to organization, technical content, format, etc.) \_\_\_\_\_  
\_\_\_\_\_  
\_\_\_\_\_

CURRENT ADDRESS

Organization \_\_\_\_\_  
Name \_\_\_\_\_ E-mail Name \_\_\_\_\_  
Street or P.O. Box No. \_\_\_\_\_  
City, State, Zip Code \_\_\_\_\_

7. If indicating a Change of Address or Address Correction, please provide the Current or Correct address above and the Old or Incorrect address below.

OLD ADDRESS

Organization \_\_\_\_\_  
Name \_\_\_\_\_  
Street or P.O. Box No. \_\_\_\_\_  
City, State, Zip Code \_\_\_\_\_

---

DEPARTMENT OF THE ARMY

OFFICIAL BUSINESS

**BUSINESS REPLY MAIL**  
FIRST CLASS PERMIT NO 0001,APG,MD

POSTAGE WILL BE PAID BY ADDRESSEE

DIRECTOR  
US ARMY RESEARCH LABORATORY  
ATTN AMSRL WM BD  
ABERDEEN PROVING GROUND MD 21005-5066



NO POSTAGE  
NECESSARY  
IF MAILED  
IN THE  
UNITED STATES

